Jose-Manuel Fernández González, Pablo Padilla,
Juan F. Valenzuela-Valdés, Jose-Luis Padilla,
and Manuel Sierra-Pérez

An Embedded Lightweight Folded Printed Quadrifilar Helix Antenna

UAV telemetry and remote control systems.

An embedded folded, printed, quadrifilar helix antenna (FPQHA) with a wide-angle coverage for unmanned aerial vehicles (UAVs) telemetry and remote control systems is presented in this article. The novelty of this design is that the FPQHA needs to be designed carefully due to UAV tail dimensions and weight constraints while maintaining a high performance to be integrated in the inner part of the UAV tail fuselage to reduce aerodynamic drag. The radiating terminal, formed by a folded, printed, four-helix, radiating section and a compact feeding network, is designed to provide left-handed, circular polarization (LHCP). The complete design offers a very homogeneous pattern in azimuth with a very good axial-ratio (AR) level over a wide range of elevation angles. The use of low-loss and lightweight materials is also an advantage of this design. The wide radiation pattern favors its use for multielement communication systems. Finally, the antenna performance results are obtained mounted inside a UAV tail platform.

UNMANNED AERIAL VEHICLES

The recent advances in wireless communication systems regarding either the radiating terminals or the radio frequency devices in the transmission and reception systems have enabled new possible applications and services. One of these new applications is the development of communication systems for UAVs [1]. A UAV refers to any aircraft that is capable of flying in an autonomous way and operating in a wide range of missions and emergency scenarios. The UAVs can either be remotely controlled from a ground base station, or they may have no necessity of human intervention, being piloted by an embedded computer (a flight control system). Whatever the nature of the UAV, its elements, such as its sensors, global positioning system (GPS), servos, and communication systems, are vital to its remote or autonomous operation [2]. After many years of development, UAVs are reaching the crucial moment in which they could be applied in a civil or military scenario. There is a huge amount of potential applications and services emerging for UAV use: remote environmental or agricultural monitoring, pollution assessment, fire prevention, security or military purposes, and communication system deployment of communication systems, among others. In regard to communication systems, the breaking idea is to reuse UAVs for communication networks so that they can be easily deployed as node relays to extend coverage and guarantee the network connectivity and quality of service [3]. However, one of the main limitations of the UAV is that it lacks the hardware and software support to effectively develop such potentialities. This is especially important for the communication system because the set of devices (transmitters, receivers, controllers, radio modems,

Digital Object Identifier 10.1109/MAP.2017.2686702
Date of publication: 26 April 2017

microwave links, and more) has to guarantee the continuous link between the UAV and the base station.

In many cases, the UAV communication systems are habitually joined to satellite communication links. Some examples are navigation applications using any GPS or low–Earth-orbit (LEO) communication satellite networks. This last one will play a promising role, not only in UAV communication links and services, but also in the introduction of UAVs in LEO satellite networks for data relaying applications, increasing the potential communication range of such satellite systems [4].

Regarding the antenna terminals, the emergence of these new UAV communication systems have led to the development of embedded devices. All those satellite systems particularly require terminals exhibiting excellent AR levels, large bandwidth, and wide beamwidth, habitually with circular polarizations (CPs). Additionally, the particular design requirements in UAVs are of paramount importance, mainly related to lightweight materials, pattern requirements, device integration, mounting platform restrictions, electromagnetic compatibility, interference compliance requirements, or others. Useful antenna configurations that satisfy most of these requirements are printed, stacked, patch antennas; cross-printed dipoles; or quadrifilar helix antennas (QHAs) [5] [6]. The advantage of a FPQHA over a wired QHA or a classical printed QHA (PQHA) is that it offers the advantage of size reduction, wider bandwidth, wider circularly polarized beam, lightweight, low cost, and ease of fabrication [7]–[11]. Also, the meander line technique can be used for PQHA size reduction [12].

In this article, an embedded FPQHA mounted in a UAV tail platform is proposed, designed, and measured. The main contribution of this article is the FPQHA design due to the dimension and weight constraints imposed by the UAV tail while maintaining a very good AR performance over a wide range of elevation angles. The integration of the FPQHA in the inner part of the UAV tail fuselage to reduce aerodynamic drag and the compact feeding network are also a challenge. The advantage of the FPQHA for UAV telemetry and remote control systems is the omnidirectional azimuth coverage with a very good AR performance over a wide range of elevation angles to communicate with the satellite communications links or UAV ground control unit.

FPQHA DESIGN AND SIMULATION

In this section, the antenna structure, the design details, and the simulation results of the FPQHA are provided. The simulation results obtained in the design process are also presented. The system requirements are provided in Table 1. The requirement of the FPQHA bandwidth is 0.865–0.871 GHz for UAV telemetry and remote control systems. The center frequency (0.868 GHz) is chosen as the design frequency. The antenna is formed by a four-helices radiating section and a compact feeding network, which provides the LHCP. Figure 1 provides detailed views of the FPQHA design, showing a three-dimensional (3-D), computer-aided-design view [Figure 1(a)] and the unwrapped helix-based structure [Figure 1(b)].

After an iterative optimization process using a transient solver in CST Microwave Studio, the final design parameters and dimensions are obtained (Table 2), considering the dimension and weight constraints. The computational resources used to achieve this objective are an Intel Xeon central processing unit X5677 with 3.47 GHz (two processors, four cores, and eight threads) and 24 GB random-access memory. This design is based on [6]. This final design is

TABLE 1. THE FPQHA SPECIFICATIONS.

Parameter	FPQHA	Units
Frequency	0.865–0.871	GHz
Polarization	LHCP	-
AR	< 3	dB
3 dB beamwidth in elevation	180 (–90 to 90)	°
Radiation pattern in azimuth	Omnidirectional	°
Cross-polarization discrimination	> 15.3	dB
Gain	> 2.5	dB
VSWR	1.4:1 (–15.6 dB)	–
Impedance	50	Ω
Maximum radius	< 13.5	mm
Maximum length	< 230	mm
Maximum weight	< 15	g

VSWR: voltage standing-wave ratio.

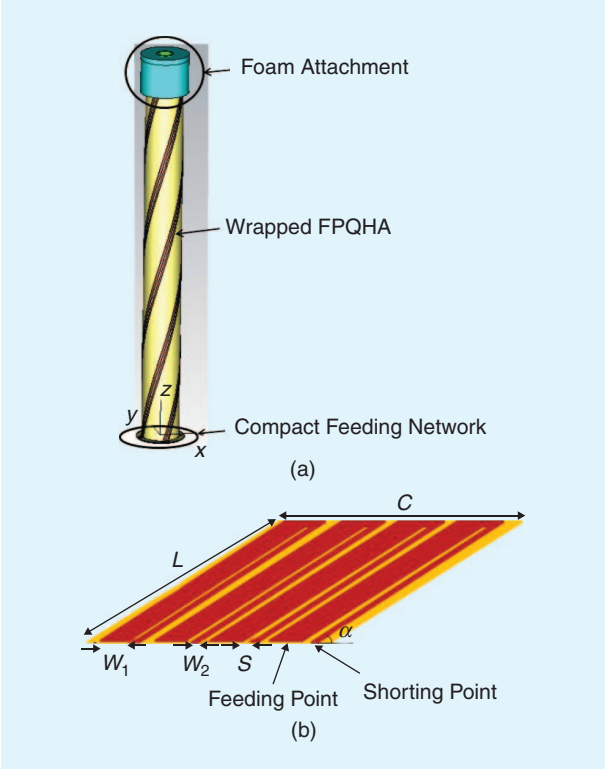

FIGURE 1. The details of the FPQHA structure: (a) the complete view of the antenna and (b) the unwrapped FPQHA structure.

TABLE 2. THE DESIGN PARAMETERS AND DIMENSIONS.

Parameter	Value	Units
Antenna substrate height (h)	0.127	mm
Antenna substrate permittivity (ε_r)	2.17	—
Circumference (C)	69.1	mm
Strip length (L)	238.4	mm
Conductor strip width (W_1)	1.5	mm
Parasitic strip width (W_2)	1	mm
Gap between conductor and parasitic strip (S)	1	mm
Number of helix turns (N)	1	—
Pitch angle (α)	74°	°
Filar input impedance	50	Ω
Feeding network substrate height (h_2)	0.4	mm
Feeding network substrate permittivity (ε_r)	4.7	—
Feeding network impedance	50	Ω
Weight	12	g
Cost	40	€

obtained in terms of restricted radius, weight, and a compact feeding network integrated in the inner part of the UAV tail fuselage while maintaining a high performance.

The structure model with its simulated 3-D radiation pattern is shown in Figure 2. The figure illustrates the axial-mode radiation of the FPQHA: the forward helix mode (endfire radiation). Figure 3 shows the main radiation pattern results of the design in azimuth and elevation for LHCPs. Figure 4 displays the AR versus the theta variation of the forward (LHCP). The FPQHA produces a nearly hemispherical radiation pattern with a very good AR performance over a wide range of elevation angles.

FPQHA PROTOTYPE INTEGRATION AND MEASUREMENT RESULTS

The antenna design is built and integrated inside the UAV tail fuselage and measured in the spherical anechoic measuring facility of the Radiation Group of the Technical University of Madrid, Spain, to validate its working features. This section describes building details of the prototype (Figure 5). The measurements carried out in the anechoic system include: the antenna radiation pattern, the AR versus theta and versus frequency, the gain, and the S-parameters.

Figure 5(a) shows where the FPQHA is located in the UAV tail fuselage. The wrapped FPQHA-based structure is linked to the compact feeding network by soldering the

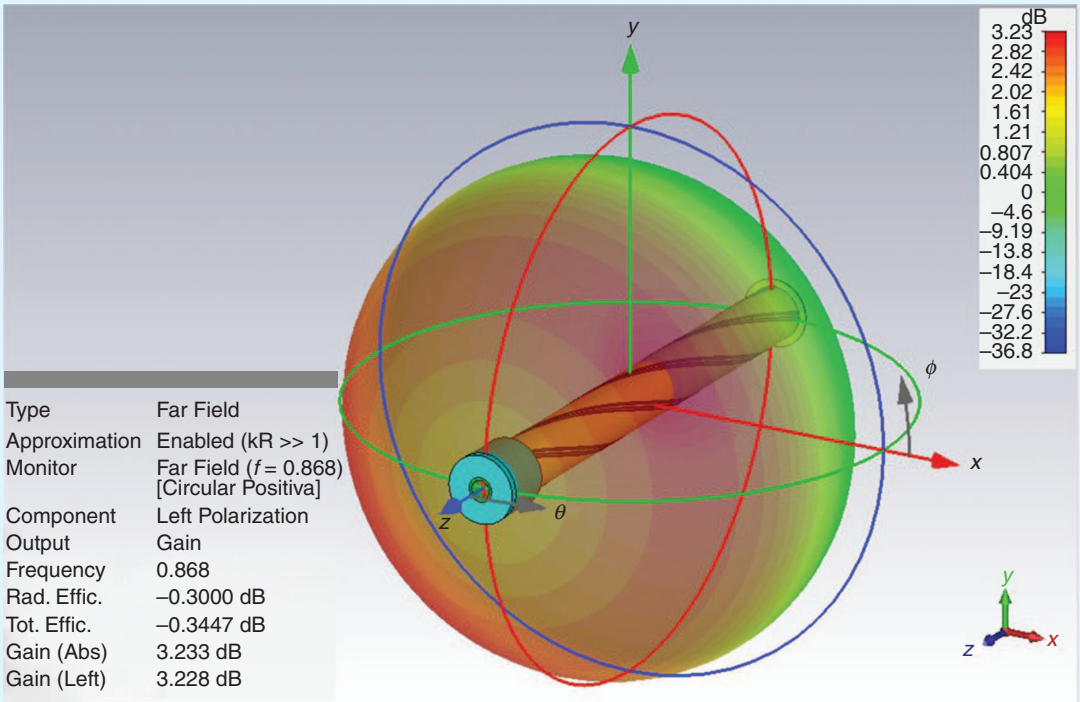

FIGURE 2. The radiation pattern in 3-D of the FPQHA simulation model for LHCP—the endfire radiation in axial mode.

feeding points and the shorting points, respectively. The LHCP, 50-Ω, subminiature version A connector is depicted too. The four-helices radiating elements are printed on a polytetrafluoroethylene Nelco NY9217 substrate of dielectric constant of $\varepsilon_r = 2.17$, loss tangent of $\tan\delta = 0.0008$, density of 2.23 g/cm^3, and thickness of $h = 0.127$ mm with a top copper foil of 35 μm. The foam attachments are manufactured on a low-density, lightweight ROHACELL HF 51 foam substrate of $\varepsilon_r = 1.057$, loss tangent of $\tan\delta = 0.0002$, density of 0.032 g/cm^3, and thickness of $h = 3$ mm. They allow the radius constraint of the wrapped FPQHA-based structure to fit inside the UAV tail fiberglass fuselage.

Figure 5(b) details the compact CP feeding network design scheme with LHCP input and four output ports (feeding points). The antenna can be excited in each feeding point in terms of phase to get the LHCP. When the input port is the LHCP, the phase excitation of the conductor strips is 0°, 90°, 180°, and 270° in the counterclockwise direction. Consequently, the LHCP in endfire radiation mode is obtained (see Figure 2). The feeding network is done in a FR-4 printed circuit board of thickness $h_2 = 0.4$ mm with compact commercial 90° hybrid circuits from Mini-Circuits at an ultrahigh frequency (UHF) band. The UAV tail fuselage composite is made of fiberglass, and the structural features, such as the joints, access hatches, tail boom, propelling blades, and push-pull connectors, have a very small influence on the antenna performance at the 0.868-GHz band. The UAV tail fiberglass fuselage is considered during the design process. Figures 5 and 6 provide some details of the antenna integration and its measuring setup.

Figure 7 offers the LHCP port reflection coefficient of the FPQHA fit inside the UAV tail fuselage. The criterion of voltage standing-wave ratio (VSWR) is satisfied in a wider band than the specified UHF operating band. The measured bandwidth, for a VSWR < 1.4, is about 34.5%.

The antenna performance in terms of radiation pattern is provided in Figure 8 for azimuth and elevation. The figures depict the measured pattern of the FPQHA prototype integrated in the inner part of the UAV tail fiberglass fuselage for LHCP input.

Figure 3 shows that the measured pattern adequately matches the expected one. The effect of the UAV tail fiberglass fuselage has a small influence on the antenna performance. Figure 9 shows the measured AR versus frequency in $\theta = 0°$, $\theta = 45°$, and $\theta = 90°$ (elevation) for the LHCP (endfire radiation). The measured results show that the AR is satisfied in a wider band than the specified operating band. Figure 10 illustrates the measured AR versus θ variation (elevation) of the FPQHA prototype inside the UAV tail platform at 0.868 GHz for the LHCP. The plots show a very good AR (AR < 3 dB) level of the FPQHA over a wide range of elevation angles for the LHCP (forward helix mode).

Table 3 compares the antenna specifications with the measured results inside the UAV tail fuselage. The measurement results fulfill completely the antenna requirements. The gain measurement versus frequency for the LHCP is presented in Figure 11. A very good agreement is observed, and the design process of the FPQHA is validated. Table 4 provides the simulated and measured gain and directivity values of the FPQHA.

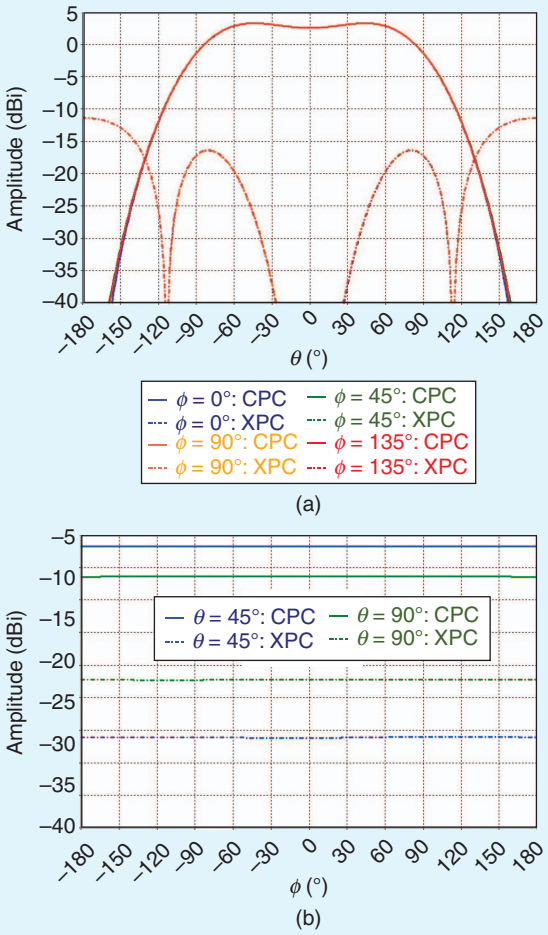

FIGURE 3. The simulated radiation pattern of the FPQHA structure at 0.868 GHz for LHCP (endfire radiation): (a) for $\phi = 0°$, $\phi = 45°$, $\phi = 90°$, and $\phi = 135°$ (azimuth) and (b) for $\theta = +45°$ and $\theta = +90°$ (elevation). CPC: copolarization component; XPC: cross-polarization component.

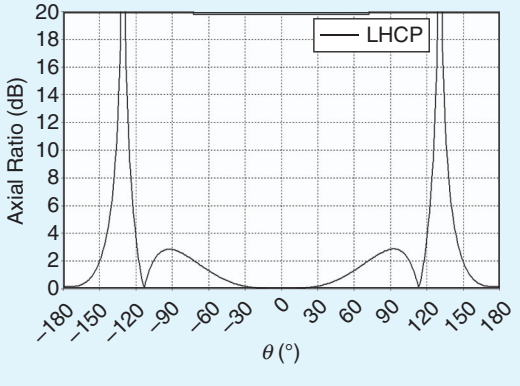

FIGURE 4. The AR versus the elevation angle of the FPQHA simulation model for LHCP (endfire radiation).

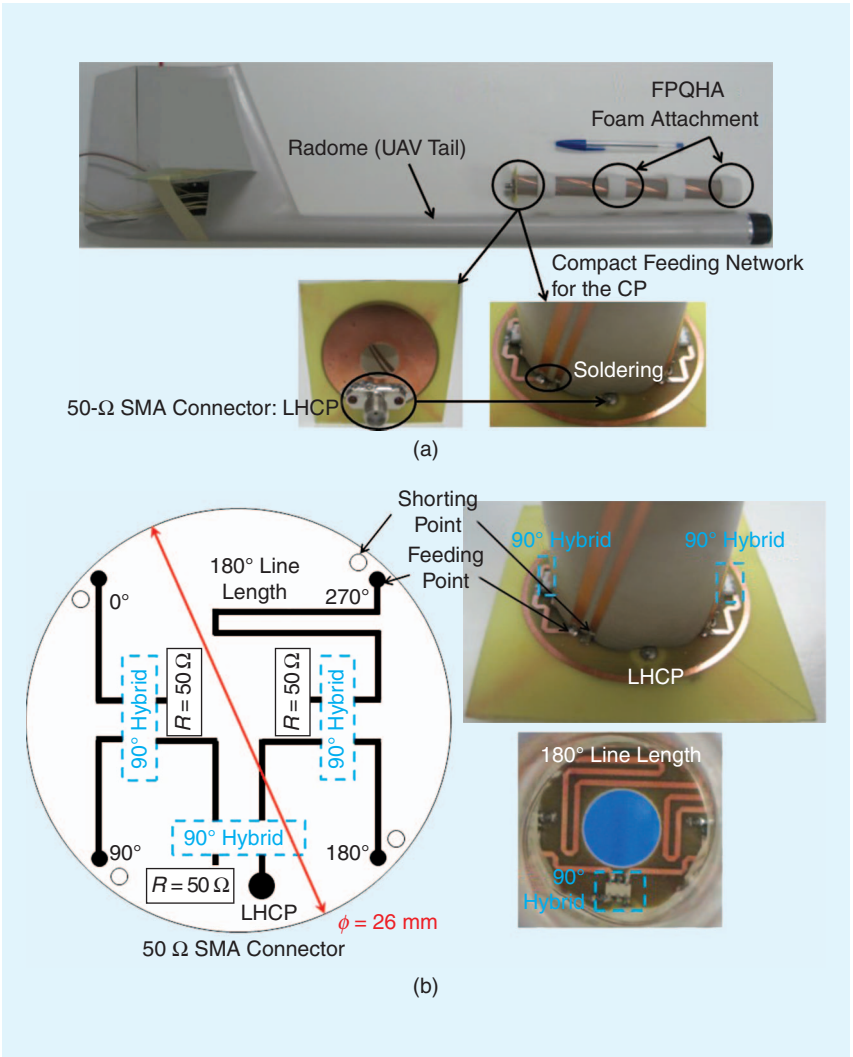

FIGURE 5. The details of the FPQHA prototype integration: (a) the FPQHA prototype with UAV tail fiberglass fuselage and (b) the compact feeding network to get the LHCP. SMA: subminiature.

Only very small discrepancies between the simulation and the measurements are observed. The complete design offers a compact structure and a very homogeneous pattern in azimuth with a very high efficiency considering the use of low-loss materials. Additionally, the weight and costs of such a design are quite reduced compared to other antenna options.

CONCLUSIONS

This article proposed and presented an embedded FPQHA with wide-angle coverage integrated inside the UAV tail fuselage at the UHF band for UAV telemetry and remote control systems. The proposed design was studied through electromagnetic simulations and validated by means of a prototype. During the design process, a UAV tail fiberglass fuselage was considered, and the antenna performance characteristics of the prototype were measured and analyzed. The results properly matched the theoretical performance in the specified frequency band. Thus, the agreement of the experimental results with the simulation outcomes indicates the validity of the analysis, design, fabrication, and integration of this antenna inside a UAV tail fuselage. The antenna was formed by a printed, four-helices radiating section and a compact feeding network, which provides CP.

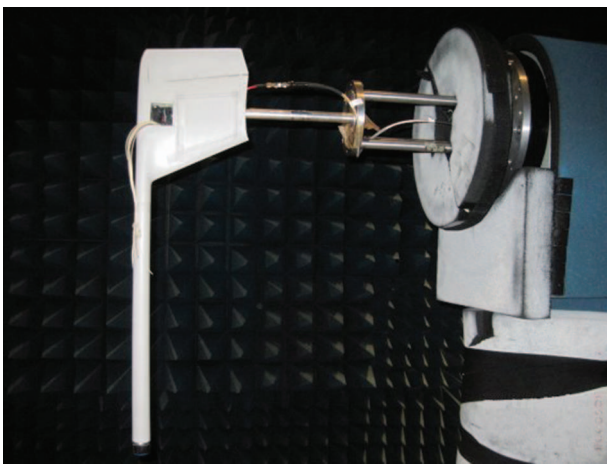

FIGURE 6. The measurement setup for the FPQHA prototype integrated inside the UAV tail fuselage in the anechoic chamber at the Technical University of Madrid.

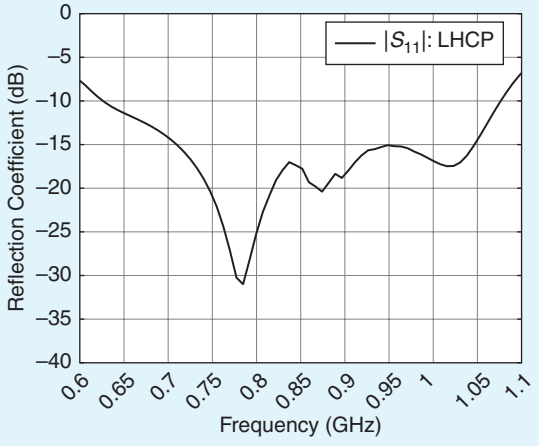

FIGURE 7. The FPQHA prototype inside the UAV tail fuselage: $|S_{11}|$ measurement.

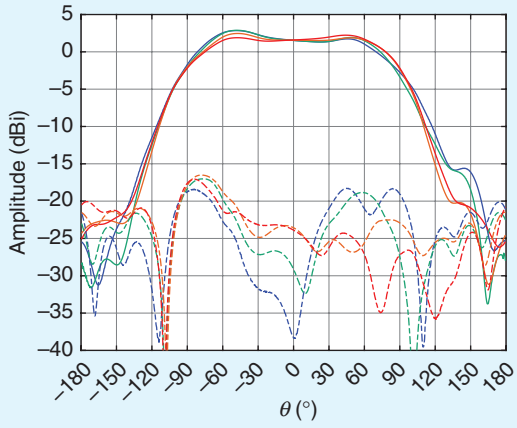

(a)

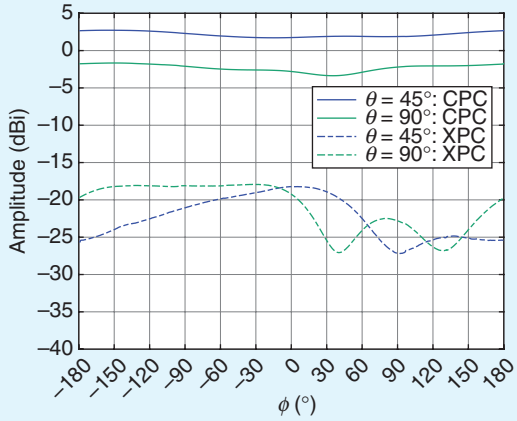

(b)

FIGURE 8. The measured radiation pattern of the PQHA prototype inside the UAV tail fuselage at 0.868 GHz for LHCP (endfire radiation): (a) for $\phi = 0^\circ$, $\phi = 45^\circ$, $\phi = 90^\circ$, and $\phi = 135^\circ$ (azimuth) and (b) for $\theta = +45^\circ$ and $\theta = +90^\circ$ (elevation).

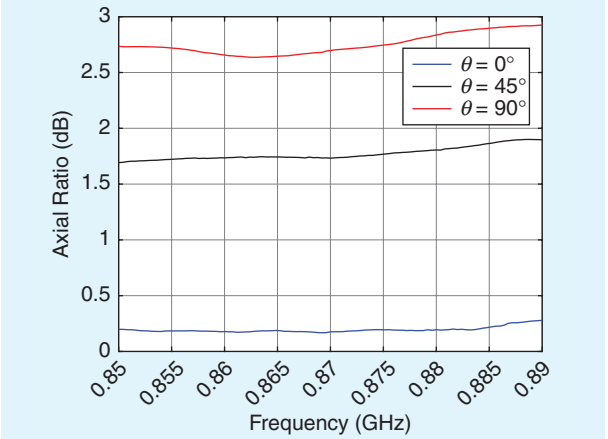

FIGURE 9. The AR measurement versus the frequency in $\theta = 0^\circ$, $\theta = 45^\circ$ and $\theta = 90^\circ$ (elevation) of the FPQHA prototype inside the UAV tail fuselage for LHCP.

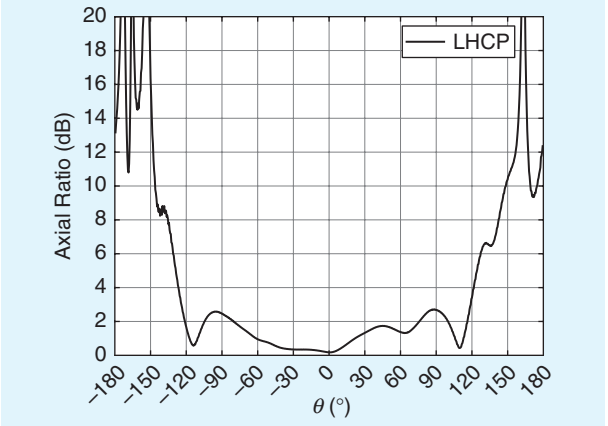

FIGURE 10. The AR measurement versus π variation (elevation) of the FPQHA prototype inside the UAV tail fuselage for LHCP at 0.868 GHz.

The main contribution of this article is the FPQHA design due to the dimension and weight constraints imposed by the UAV tail while maintaining an exceptional AR performance over a wide range of elevation angles. The integration of the FPQHA in the inner part of the UAV tail fuselage to reduce aerodynamic drag and the compact feeding network are also a challenge. Furthermore, the advantage of this FPQHA for UAV telemetry and remote control systems is the omnidirectional azimuth coverage with a very good AR performance over a wide range of elevation angles to communicate with the satellite communication links or the UAV ground control unit. This FPQHA needed to be carefully designed due to dimensions and weight constraints while maintaining a high performance to fit inside the UAV tail fuselage. This compact, lightweight, and low-cost manufacturing process configuration makes the design suitable for its integration in aircrafts fuselage.

ACKNOWLEDGMENTS

We sincerely thank P. Caballero Almena and C. Martinez Portas for their assistance with measurements in the anechoic chamber at the Technical University of Madrid.

The simulations done in this work have been carried out using CST Studio Suite under a cooperation agreement between Computer Simulation Technology and Universidad Politécnica de Madrid. This work has been supported by the project ENABLING5G, "Enabling Innovative Radio Technologies for 5G networks" (TEC2014-55735-C3-1-R) of the Spanish Research and Development National Program and by the project S2013/ICE-3000 SPADERADAR-CM of the Madrid Region Government.

TABLE 3. A COMPARISON BETWEEN FPQHA SPECIFICATIONS WITH MEASUREMENTS INSIDE THE UAV TAIL FUSELAGE.

Parameter	Specifications	Measurements	Units
Frequency	0.865–0.871	0.85–0.89	GHz
Polarization	LHCP	LHCP	–
AR	< 3	< 3 (–122° to 120°)	dB
3 dB beamwidth in elevation	180 (–90 to 90)	180 (–90 to 90)	°
Radiation pattern in azimuth	Omnidirectional	Omnidirectional	°
Cross-polarization discrimination	> 15.3	17	dB
Gain	> 2.5	2.6	dB
VSWR	1.4:1 (–15.6 dB)	1.4:1 (–15.6 dB)	–
Impedance	50	50	Ω
Maximum radius	< 13.5	11	mm
Maximum length	< 230	229.2	mm
Maximum weight	< 15	12	g

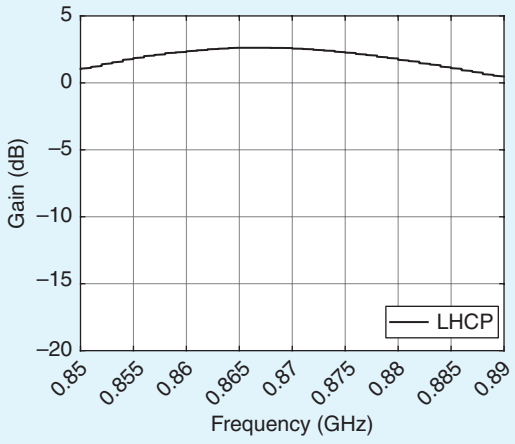

FIGURE 11. The gain measurement versus the frequency of the embedded FPQHA prototype inside the UAV tail fuselage for LHCP.

TABLE 4. THE GAIN AND DIRECTIVITY FOR LHCP AT 0.868 GHz: MEASUREMENTS VERSUS SIMULATION.

	Gain [dB]		Directivity [dBi]	
	Simul.	Meas.	Simul.	Meas.
LHCP	3.2	2.6	3.5	3.2

AUTHOR INFORMATION

Jose-Manuel Fernández González (jmfdez@gr.ssr.upm.es) received his Diplôme d'Ingénieur en Électricité from the École Polytechnique Fédérale de Lausanne, Switzerland, in 2003 and his Ph.D. degree from the Universidad Politécnica de Madrid, Spain, in 2009. Since 2013, he has been an assistant professor at the Universidad Politécnica de Madrid. His current research interests are phased-array antennas, radio frequency circuits, and metamaterial structures with emphasis on planar antenna applications.

Pablo Padilla (pablopadilla@ugr.es) received his telecommunication engineer degree from the Technical University of Madrid, Spain, in 2005. Since 2012, he has been an associate professor at the Universidad de Granada, Spain. His research interests include radio frequency devices, antennas, propagation, wireless communication networks, and data exploration.

Juan F. Valenzuela-Valdés (juanvalenzuela@ugr.es) received his degree in telecommunications engineering from the Universidad de Malaga, Spain, in 2003 and his Ph.D. degree from the Universidad Politécnica de Cartagena, Spain, in 2008. In 2015, he joined the Universidad de Granada as an associate professor. His research areas cover wireless communications and efficiency in wireless sensor networks.

Jose-Luis Padilla (jluispt@ugr.es) received his B.Sc. degree in physics in 2003, his M.A.S. degree in theoretical physics in 2005, and his Ph.D. degree in 2012, all from the University of Granada, Spain. He is currently a fellow of the Marie Curie Programme with the University of Granada. His current research interests include nanoelectronics with special interest in theoretical modeling and simulation of semiconductor devices.

Manuel Sierra-Pérez (m.sierra.perez@gr.ssr.upm.es) received his M.S. degree in 1975 and his Ph.D. degree in 1980 from the Universidad Politécnica de Madrid, Spain. He became a full professor at the same university in 1990. His main interest is passive and active array antennas, including design theory, measurement, and applications. He is a Senior Member of the IEEE.

REFERENCES

[1] B. T. Strojny and R. G. Rojas, "Integration of conformal GPS and VHF/UHF communication antennas for small UAV applications," in *Proc. 3rd European Conf. Antennas and Propagation*, Berlin, 2009, pp. 2488–2492.

[2] R. L. Cravey, E. Vedeler, L. Goins, R. W. Young, and R. W. Lawrence, "Structurally integrated antenna concepts for Hale UAVs," NASA Langley Research Center, Rep. NASA/TM-2006-214513, 2006.

[3] Z. Pengcheng, Y. Kai, and A. L. Swindlehurst, "Wireless relay communications with unmanned aerial vehicles: Performance and optimization," *IEEE Trans. Aerosp. Electron. Syst.*, vol. 47, no. 3, pp. 2068–2085, July 2011.

[4] D. D. Mrema and S. Shimamoto, "Performance of quadrifilar helix antenna on EAD channel model for UAV to LEO satellite link," in *Proc. Int. Conf. Collaboration Technologies Systems* 2012, pp.170–175.

[5] A. Sharaiha, C. Terret, and J. P. Blot, "Printed quadrifilar resonant helix antenna with integrated feeding network," *Electron. Lett.*, vol. 33, no. 3, pp. 256–257, Feb. 1997.

[6] Y. Letestu and A. Sharaiha, "Broadband folded printed quadrifilar helical antenna," *IEEE Trans. Antennas Propag.*, vol. 54, no. 5, pp. 1600–1603, May 2006.

[7] A. T. Adams and C. Lumjiak, "Optimization of the quadrifilar helix antenna," *IEEE Trans. Antennas Propag.*, vol. 19, no. 4, pp. 547–548, July 1971.

[8] C. C. Kilgus, "Shaped-conical radiation pattern performance of the backfire quadrifilar helix," *IEEE Trans. Antennas Propag.*, vol. 23, no. 3, pp. 392–397, May 1975.

[9] B. P. Kumar, M. Kumar, C. Kumar, V. S. Kumar, and V. V. Srinivasan, "Integrated quadrifilar helix at c-band for spacecraft omni antenna system," in *Proc. IEEE Applied Electromagnetics Conf.*, Kolkata, 2011, pp. 1–4.

[10] B. T. Stojny and R. G. Rojas, "Bifilar helix GNSS antenna for unmanned aerial vehicle applications," *IEEE Antennas Wireless Propag. Lett.*, vol. 13, pp. 1164–1167, 2014. doi: 10.1109/LAWP.2014.2322577.

[11] N. Terada and K. Kagoshima, "Backfire/endfire radiation performance of quadrifilar helical antennas," *Electron. Lett.*, vol. 27, no. 12, pp. 1108–1109, June 1991.

[12] D. K. C. Chew and S. R. Saunders, "Meander line technique for size reduction of quadrifilar helix antenna," *IEEE Antennas Wireless Propag. Lett.*, vol. 1, no. 1, pp. 109–111, 2002.